Design of a compact SOI Polarization Rotator for mid-IR application*

Ajanta Barh, Bishnu P. Pal, and R. K. Varshney
Department of Physics
Indian Institute of Technology Delhi
New Delhi 110016, India
e-mail: ajanta.barh@gmail.com

B. M. Azizur Rahman
School of Engineering and Mathematical Sciences
City University London
London EC1V 0HB, UK
e-mail: b.m.a.rahman@city.ac.uk

A*bstract*— Design of a compact polarization rotator (PR) exploiting power coupling through phase matching between the TM mode of a strip waveguide (WG) and TE mode of a vertical slot WG is presented. Optimized cross sectional dimensions of the coupler have been achieved to use this device as a compact PR at 3 μm wavelength with device length of just 2 mm. We also investigate the device performance at the operating wavelength (λ) = 1.55 μm.

Keywords-component; Polarization selective device; Si-on-insulator (SOI) waveguides; slot waveguides

I. INTRODUCTION

Silicon photonics is emerging as a low-cost technology by integrating it directly on top of a well developed CMOS platform [1, 2]. Today, silicon-based platforms support the realization of a wide variety of devices, including high-speed modulators and detectors [3], low-loss waveguides [4] and other passive and active [5], linear and non-linear [6] components. Recently, silicon on insulator (SOI)-based nano sized compact slot optical WG has assumed importance due to its potential applications [7]. Due to high index contrast at the interface, transverse electric field shows a very high discontinuity at the interface with very high optical confinement inside the low index slot region when the transverse dimension of the slot is less than the characteristic decay length of that electric field [7-9]. Though the slot and strip WG dimensions are small but they are highly polarization sensitive. However, for polarization diversity systems, this problem can be sorted out by incorporating polarization splitter and polarization rotator/converter. Recently, polarization rotator (PR) made of horizontal slot and strip WG has been reported based on mode evolution [10]. Its fabrication poses difficulty as required proper control of tapered structure is relatively difficult to realize. Moreover, it can rotate only one polarization state for one input direction. Another design of polarization splitter has been reported based on resonant tunnelling between three WGs [11]. In this paper, we propose a design for realizing a PR for potential application at the mid-IR wavelength region that should be relatively easy to fabricate as no tapering is required and the whole structure can be made with a single mask. Moreover, it can rotate both polarization states for a single input direction (i.e., at coupling length (L_c), TM input in the Si strip WG will produce TE output from the slot WG and TE input in the slot WG will produce TM output from the strip WG). In the present configuration we have shown that it is possible to match and couple two different polarization states by exploiting efficient coupling between a silicon strip WG and an air-silicon vertical slot WG.

II. METHODOLOGY

A. *Proposed Structure*

The contour map of the transverse refractive index profile of the proposed PR is shown schematically in Fig. 1. Here two WG's are implemented on silica (SiO_2) base with air as cover and low index slot material. But we can use any low index compatible materials for the slot region, such as electro-optic materials for high-speed modulators [3], doped material to achieve gain [5] or sensing material for efficient organic/inorganic sensing [12]. We have taken the same height for both the WGs as H and same width for the high index regions of the slot WG as W_2. The width of the strip WG core and low index region of slot WG are taken as W_1 and W_s, respectively. The separation between two WGs is denoted as S.

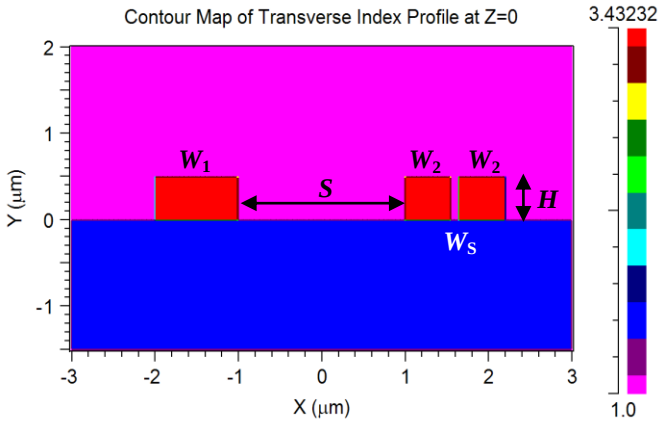

Figure 1. Schematic transverse view of refractive index profile of the PR.

B. *Numerical optimization*

A full vectorial finite element method was implemented to analyze the above mentioned 2-D structure. Abrupt refractive index change has been taken care of by optimizing the mesh. Convergence was tested by optimizing the domain boundary and the x, y grid size. All the vector fields are investigated and

* Work is partially supported by Department of the Navy Grant N62909-10-1-714 issued by Office of Naval Research Global.

depending on mode hybridness, TE and TM modes are identified. Vertical slot WG is more likely to confine TE mode (E_x is the dominant component). So, here confinement of the fundamental TE mode in slot WG and TM mode in strip WG is considered. For moderate electric field confinement in the slot, we choose W_s as 100 nm. Fabrication simplicity requires same height (H) for both WGs. Now for sufficient confinement of TM mode inside strip at 3 µm wavelength, the H should be > 400 nm. Larger H gives better results but for compactness of the overall device, one may have to sacrifice this aspect at the design stage. Thus after optimization we have fixed H at 500 nm. To find suitable W_2, we studied the effective index (n_{eff}) of TE and TM modes in the slot WG by varying W_2 (shown in Fig. 2). To maintain TE polarization as the fundamental mode, W_2 needed to be > 500 nm. Optimizing the confinement loss, W_2 was chosen to be 550 nm for H = 500 nm of the slot WG.

III. Results and Discussions

A. PR for te mid-IR of wavelength of 3 µm

Material dispersion of Si and SiO_2 are incorporated through Sellmeier formula. The optical transmittance of Si is > 50% for 2-3 mm thickness at 3 µm wavelength. The above mentioned optimized parameters for the slot WG were W_2 = 550 nm, W_s = 100 nm, H = 500 nm. In the absence of strip WG, the n_{eff} of the fundamental TE mode in this slot WG is 1.85626626 (Fig. 3). Then we have studied n_{eff} of the TM mode inside the strip WG of same height by varying its width (W_1). For W_1 = 992 nm, the n_{eff} of strip mode becomes equal to that of the slot WG mode.

For the combined coupled structure, using these optimized dimensions (i.e. W_1 = 992 nm, W_2 = 550 nm, W_s = 100 nm, H = 500 nm), the variation of n_{eff} of the two orthogonal polarized states were studied as a function of S to determine mode exchange regime. The variation of n_{eff} of TE and TM modes with WG separation (S) are shown in Fig. 4. It could be seen that the phase matching condition is achieved for $S \approx 876$ nm. The three basic parameters to study a PR are n_{eff}, hybridness and coupling length (L_c). For three different S values (800 nm, 900 nm, 1000 nm), the variation of above mentioned parameters were studied as a function of strip WG width (W_1) and the corresponding variations are shown in Figs. 5, 6 (a, b) and 7, respectively. For n_{eff} we have studied the upper and lower effective index of the combined structure. Fig. 5 clearly indicates that the value of W_1 corresponding to anti–crossing point shifts towards a higher value as S increases. Hybridness of the two modes can be defined as the ratio of the maximum values of the H_y to H_x field components for the TM and similarly H_x/H_y for the TE mode. All the peaks appear around the mode exchange regime and this peak value increases as the S decreases.

For TE mode (see Fig. 6(a)), the peak exceeds 1. Since the hybridness was defined from the peak field components rather than the average field components, anomalies may appear when their profiles are very different. Polarization coupling length of the two modes are defined as ($L_c = (\pi / |\beta_1 - \beta_2|)$) where, β_1 and β_2 are the mode propagation constants of the TE and TM modes. Here also the peaks appear at mode exchange regime but this peak L_c decreases as S decreases (Fig. 7). Thus we may conclude that mode mixing is more efficient and required device length becomes smaller at lower value of S. Values of maximum L_c and the corresponding W_1 for different values of S are tabulated in Table-I. It is clear from the table that the variation of W_1 is very small and this variation increases for smaller S value. Thus for nearly 2 mm long coupler, the complete exchange of power between the two orthogonal polarized modes is possible for S = 900 nm.

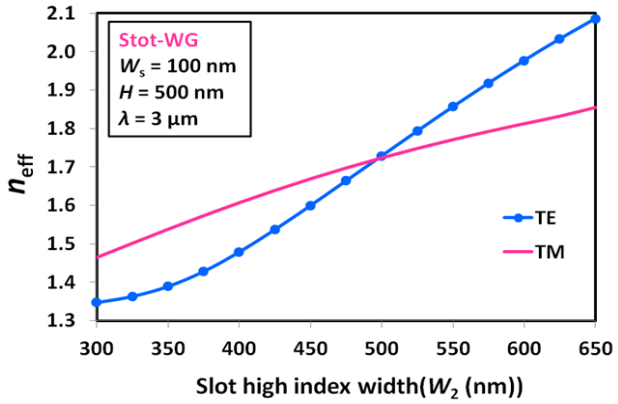

Figure 2. Variation of effective index of TE and TM mode in slot WG with the width of high index slot region (W_2).

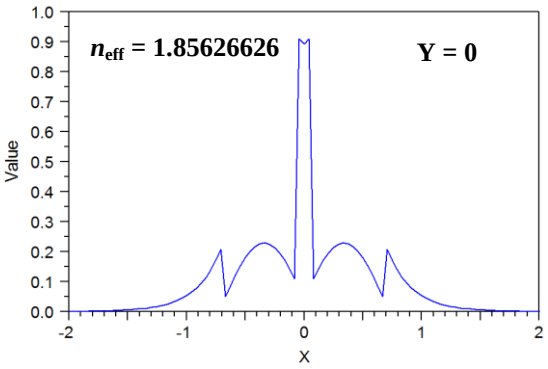

Figure 3. Horizontal cut of E_x mode profile at y = 0.

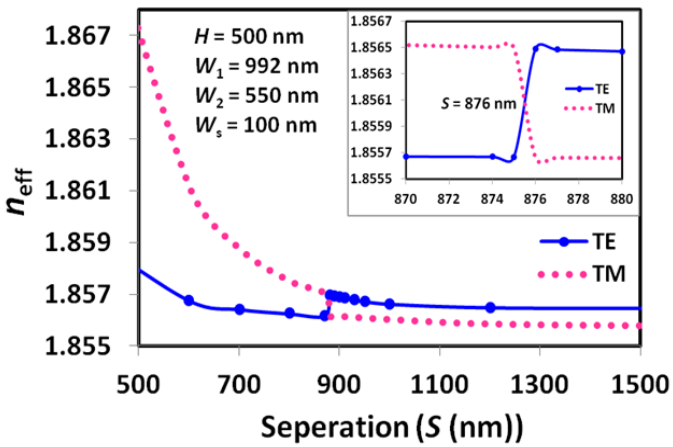

Figure 4. Variation in n_{eff} of the TE and TM modes with S. Mode exchange takes place at $S \approx 876$ nm; Inset shows enlarged view of phase matching.

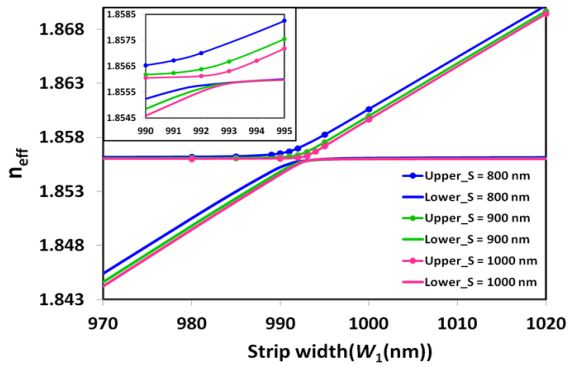

Figure 5. Upper & Lower n_{eff} variation with strip WG width (W_1) for three different S = 800 nm, 900 nm, 1000 nm; enlarge view is shown as inset.

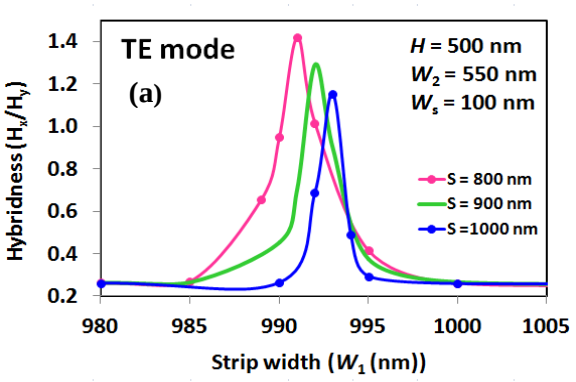

Figure 6 (a). Variation of modal hybridness of the TE mode with W_1.

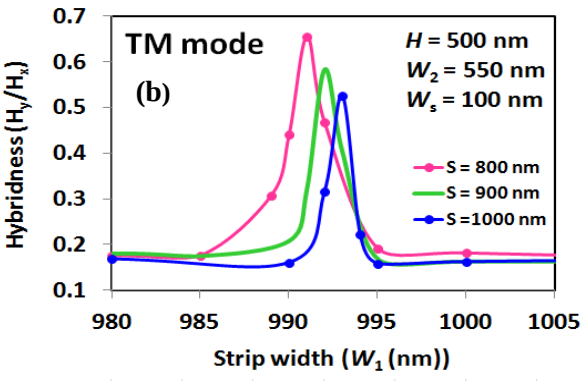

Figure 6 (b). Variation of modal hybridness of the TM mode with W_1.

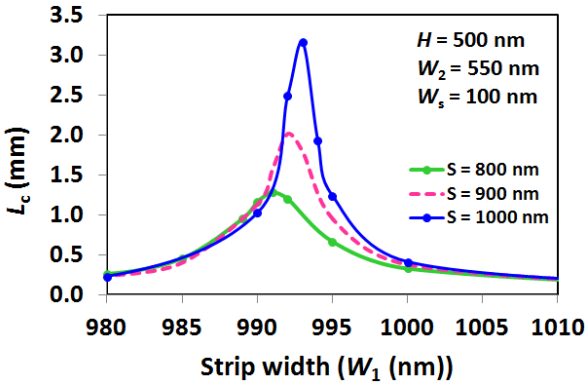

Figure 7. Variation of coupling length (L_c) with W_1.

From fabrication point of view, we have also studied the tolerance of the structure by varying the slot WG parameters (W_2, H, W_s) by ± 10%. Corresponding variations of hybridness and coupling length have been studied. Here only the L_c variations are shown in Figs. 8 (a, b, c).

TABLE I. L_C AND W_1 FOR DIFFERENT S

separation (S) (nm)	Value of phase matching L_c and W_1	
	L_c (mm)	W_1 (nm)
700	0.82	989
800	1.28	991
900	2.00	992
1000	3.15	993
1100	5.25	993.5

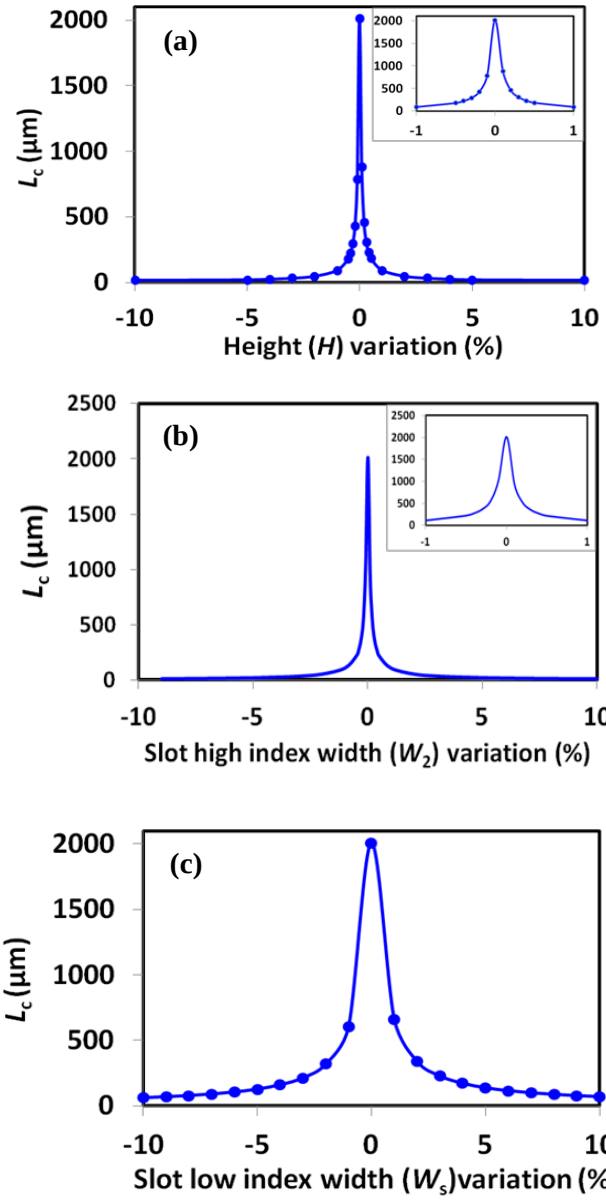

Figure 8. Tolerance study for L_c with the variation with slot parameter. (a) H variation; (b) W_2 variation; (c) W_s variation.

B. *Comparison with PR at 1.55 µm*

By shifting our operating wavelength down to 1.55 µm (today's telecommunication wavelength), the overall dimension of the PR will reduce to micron scale.

The optimized slot WG dimensions turned out to be W_2 = 255 nm, W_s = 90 nm, H = 220 nm. The values of phase matching L_c and the corresponding W_1 for different values of S are tabulated in Table-II. Unlike the previous case (i.e. operating λ = 3 µm), at the wavelength of 1.55 µm, the variation is more prominent and L_c reduces greatly. Thus at 1.55 µm for nearly 100 µm long coupler, the complete exchange of power between the two orthogonal polarized modes is possible.

TABLE II. L_C AND W_1 FOR DIFFERENT S

separation (*S*) (nm)	**Value of phase matching L_c and W_1**	
	L_c (µm)	***W_1 (nm)***
550	136.41	455
500	111.17	452
450	94.51	447

C. *Modal field plots of designed mid-IR PR at 3 µm*

Some field plots are shown below for W_2 = 550 nm, H = 500 nm, W_s = 100 nm, and W_1 = 992 nm. In Fig. 9 the TE and TM fields are plotted at mode mixing separation (S = 900 nm).

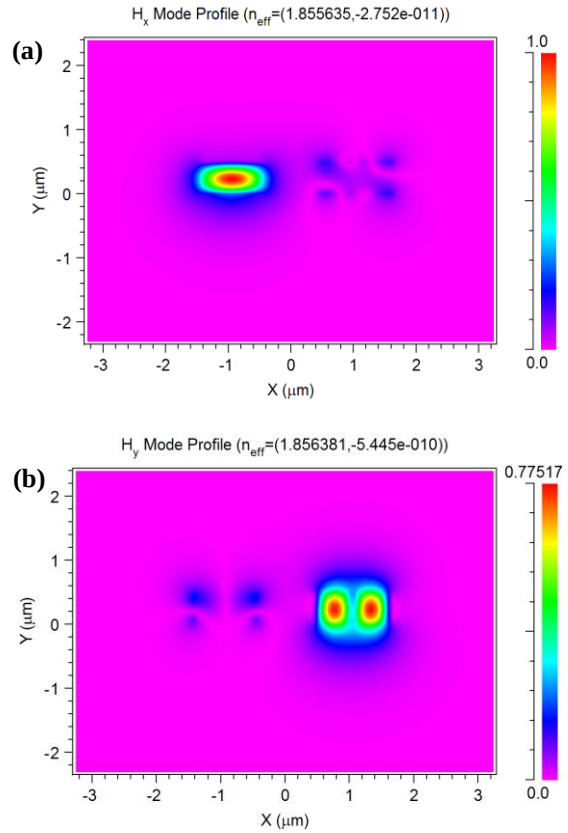

Figure 9. Modal field distribution of (a) TM_H_x (H_x>>H_y) mode in the strip WG; (b) TE_H_y (H_y>>H_x) mode in the vertical slot WG.

IV. CONCLUSIONS

A novel design of a compact SOI polarizer incorporating vertical slot waveguide is presented. The above results suggests that a PR of dimension 3.092µm x 0.5µm x 2mm can be designed for 3 µm wavelength by exploiting the phase matching between the orthogonally polarized modes of a silicon nanowire and that of a vertical slot silicon waveguide. On the other hand at 1.55 µm, a compact PR can be realized with device length below 100 µm.

ACKNOWLEDGMENT

Author A.B. gratefully acknowledges the Council of Scientific and Industrial Research (CSIR) for providing her Ph.D. fellowship.

REFERENCES

[1] B. P. Pal, "Guided wave optics on silicon: physics, technology, and status," Prog. in Optics, vol. XXXII, pp. 1-59, 1993.

[2] K. K. Lee, D. R. Lim, L. C. Kimerling, J. Shin, and F. Cerrina, "Fabrication of ultralow-loss Si/SiO_2 waveguides by roughness reduction," Opt. Lett., vol. 26, pp. 1888-1890, December 2001.

[3] T. B. Jones, M. Hochberg, G. Wang, R. Lawson, Y. Liao, P. A. Sullivan, L. Dalton, A. K. Y. Jen, and A. Scherer, "Optical modulation and detection in slotted Silicon waveguides," Opt. Express, vol. 13, pp. 5216-5226, July 2005.

[4] J. Cardenas, C. B. Poitras, J. T. Robinson, K. Preston, L. Chen, and M. Lipson, "Low loss etchless silicon photonic waveguides," Opt. Express, vol. 17, pp. 4752 – 4757, March 2009.

[5] P. Pintus, S. Faralli, and F. Di Pasquale, "Low-Threshold Pump Power and High Integration in Al_2O_3: Er^{3+} Slot Waveguide Lasers on SOI," IEEE photonics technology letters, vol. 22, pp. 1428-1430, October 2010.

[6] R. M. Osgood et al., "Engineering nonlinearities in nanoscale optical systems: physics and applications in dispersion-engineered silicon nanophotonic wires," Advances in Optics and Photonics, vol. 1, pp. 162–235, January 2009.

[7] V. R. Almeida, Q. Xu, C. A. Barrios, R. R. Panepucci, and M. Lipson, "Guiding and confining light in void nanostructure," Opt. Lett., vol. 29, pp. 1209-1211, June 2004.

[8] Q. Xu, V. R. Almeida, R. R. Panepicci, and M. Lipson, "Experimental demonstration of guiding and confining light in nanometer-size low-refractive-index material," Opt. Lett., vol. 29, pp. 1626-1628, July 2004.

[9] N. N. Feng, J. Michel and L. C. Kimerling, "Optical Field Concentration in Low Index Waveguides," IEEE journal of quantum electronics, vol. 42, pp. 885 – 890, September 2006.

[10] N. N. Feng, R. Sun, J. Michel, and L. C. Kimerling, "Low-loss compact-size slotted waveguide polarization rotator and transformer," Opt. Lett. vol. 32, pp. 2131- 2133, August 2007.

[11] M. Komatsu, K. Saitoh, and M. Koshiba, "Design of miniaturized silicon wire and slot waveguide polarization splitter based on a resonant tunneling," Optics Express, vol. 17, pp. 19225–19234, October 2009.

[12] C. A. Barrios, "Optical Slot-Waveguide Based Biochemical Sensors-Review," Sensors, vol. 9, pp. 4751-4765, June 2009.